



Range verification in heavy-ion therapy with a Hadron Tumour Marker (HTM)

E. KASANDA¹, J. EASTER¹, D. HYMERS¹, V. BILDSTEIN¹, A. SPYROU², A. RICHARDS², C. HOEHR³, D. MUECHER^{1,3}

1. University of Guelph, Canada
2. National Superconducting Cyclotron Laboratory, Michigan State University, East Lansing, MI
3. TRIUMF, Vancouver, Canada



INTRODUCTION

Heavy-ion therapy has the potential to provide near-optimal tumour coverage while sparing even more healthy bystander tissue than proton therapy¹. Figure 1 compares dose profiles for photons, protons, and heavy ions. The lack of an energy-dependent exit dose in heavy-ion therapy makes it challenging to verify the treatment quality in real time². HTM range verification (HTM RV) is a method of in vivo range verification that has been shown

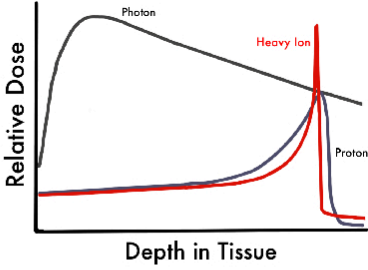


Figure 1. Illustration of dose profiles for photons, protons, and heavy ions

through simulation³ and preliminary experiments⁴ to provide accurate reconstruction of proton beam range on a sub-mm scale. In this work we present the preliminary results of the first application of HTM RV using a heavy-ion beam.

METHOD

A hadron tumour marker (HTM) is a small metallic fiducial marker that is implanted near the clinical treatment volume (CTV) to provide real time feedback on treatment quality. An HTM must be composed of a material which upon interaction with the treatment beam, undergoes two or more competing reactions whose products decay by emission of strong gamma rays within the time frame of fraction delivery. These constraints limit the available materials. Therefore, it can be advantageous to combine multiple isotopes to form a composite HTM (cHTM), using the strongest reaction channel from each isotope. HTM RV relies on the detection of characteristic gamma rays emitted through the decay of different reaction products generated by interactions between the HTM and the treatment beam. Since the gamma rays of interest are produced from competing reaction channels, the ratio of their intensities is indicative of the energy of the beam at the HTM's position, in vivo, and in real time. The use of multiple reactions with different energy dependencies allows HTM RV to be independent of detector efficiency and beam intensity. A conceptual sketch illustrating the application of HTM RV in proton therapy is illustrated in Figure 2.

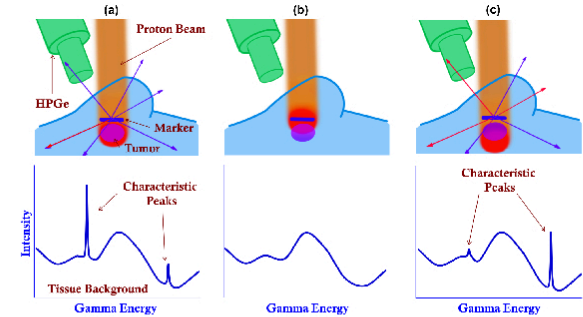


Figure 2. Concept sketch for application of HTM RV in proton therapy³. In (a), the treatment is delivered according to plan. In (b), the treatment beam undershoots the CTV. The characteristic peaks are not present. In (c), the treatment beam overshoots the CTV. The characteristic peaks are present in different relative intensities than in (a).

Since particle stopping powers scale with Z^2 , heavy ion beams have a higher energy loss rate than protons in the Bragg peak, resulting in a much stronger correlation between beam energy at the HTM position and residual range. This property is favorable for HTM RV, as the intensity of the peaks of interest will change more dramatically with a small deviation in beam range.

EXPERIMENT

In March 2020, an experiment was performed at the National Superconducting Cyclotron Laboratory (NSCL) with the goal of illustrating the application of HTM RV to heavy-ion therapy, using a 150 MeV/u ^{16}O beam. Although ^{16}O is not currently used clinically for heavy-ion therapy, there is evidence for its application using similar setups⁶. Prior to the experiment, simulations using a ^{16}O projectile on various targets were performed using PACE⁷ in order to identify potential HTM candidates. One of these candidates is ^{107}Ag , which undergoes two reactions suitable for HTM RV. The cross sections for these reactions according to PACE data are shown in Figure 3, and partial decay radiation information for the resulting reaction products is shown in Table 1.

| Isotope | Half-life (s) | γ -ray energy (keV) | γ -ray intensity (%) |
|-------------------|---------------|----------------------------|-----------------------------|
| ^{112}Sb | 53.5 | 1256.69 | 93.14 |
| ^{114}Sb | 209.4 | 1299.92 | 98.70 |

Table 1. Relevant decay radiation for reaction products of interest⁸.

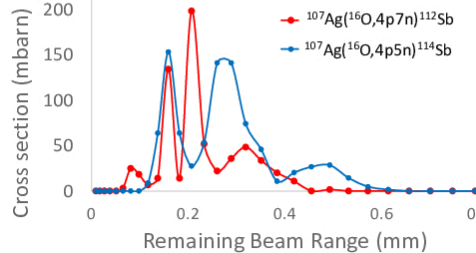


Figure 3. Cross sections for two reactions of interest in ^{107}Ag upon interaction with ^{16}O , as a function of the ^{16}O ion's remaining range in PMMA.

Several candidate HTM materials were investigated using the setup illustrated in Figure 4. The beam was slowed to the desired energy range in a block of PMMA (51 x 51 x 28 mm³) containing an HTM foil (Figure 5). The range of the beam within the PMMA was modified using a rotating aluminum degrader in the beamline. In order to acquire reference data, some targets instead consisted of an HTM foil on an Al frame, with the PMMA block positioned upstream to slow the beam to the correct energy range without contributing to the gamma background.

The emitted gammas were measured by a pair of high purity germanium (HPGe) detectors, shown in Figure 5. A rail system perpendicular to the beamline was used in order to protect the detectors from the high gamma and neutron flux present during target activation. The targets were activated for 150 seconds, then quickly moved approximately 1.5 m to be positioned in between the detectors for a decay measurement (approx. 300s).

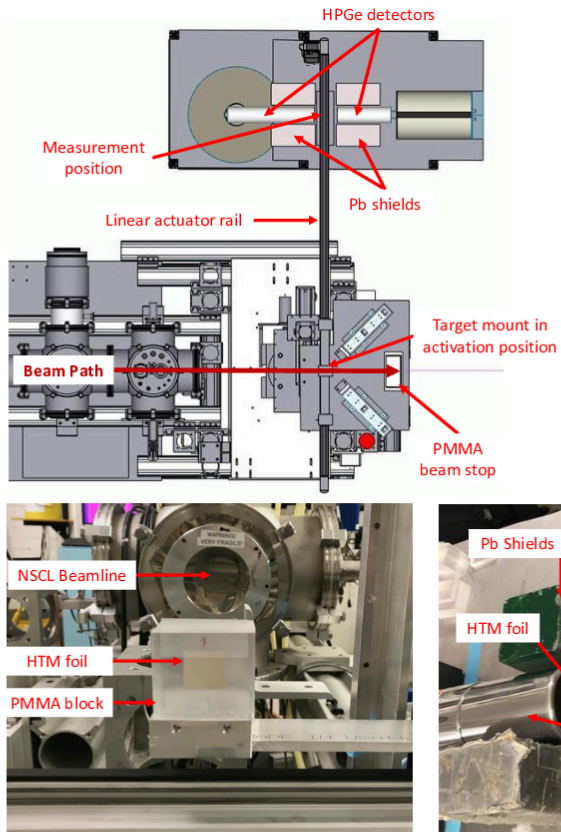


Figure 4. Sketch of experimental setup. HTM foil targets (either on a Al frame, or in PMMA) are activated in indicated activation position, then moved to measurement position between HPGe detectors to acquire a decay measurement of HTM reaction products.

Figure 5. Pictures from experiment. PMMA target containing HTM foil in activation position (left). Foil target on aluminium backing, without PMMA, in measurement position between two lead-shielded HPGe detectors (right).

PRELIMINARY RESULTS

Gamma spectra from the decay measurements of a 25 μm -thick ^{nat}Ag HTM foil mounted on an Al frame (i.e without PMMA background) are shown in Figures 6 and 7. The remaining range of the beam in PMMA after the foil for each run was calculated based on the thickness of the degraders used, with SRIM⁹ simulation data. The gamma spectra have been scaled such that the background for each run is aligned. In Figure 6, prominent background peaks are identified in grey, and the light blue square indicates the energy region that is shown in Figure 7. The indicated peaks of interest are emitted from the decay of fusion evaporation reaction products of interest (Table 1). The absolute and relative intensity of the indicated peaks varies significantly with sub-mm differences in beam range. Based on previous experiments⁴, this suggests that ^{nat}Ag is viable for further investigation as an HTM material.

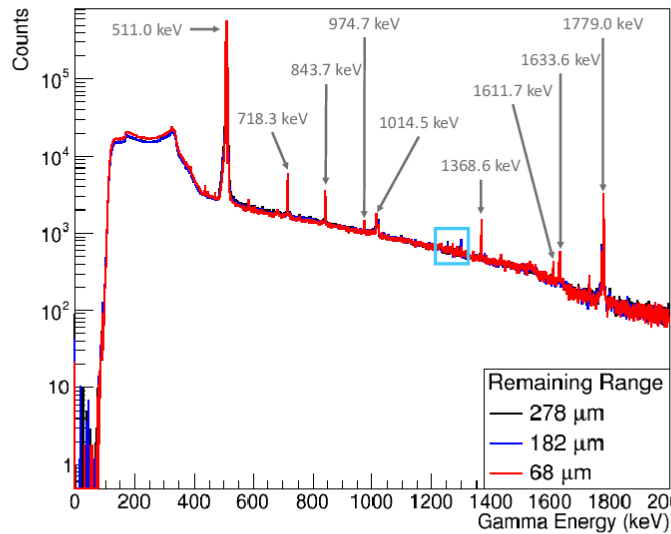


Figure 6. Selected gamma decay spectra for three different beam range settings, impinging on a 25 μm -thick ^{nat}Ag foil. Prominent background peaks are labelled in grey, and the region containing the peaks of interest is indicated by the light blue square.

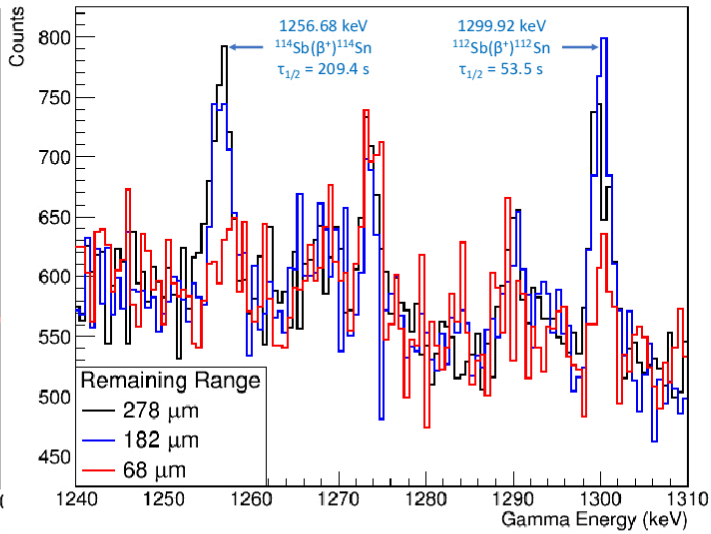


Figure 7. Region of interest from gamma decay spectra depicted in Figure 6. The peaks of interest from the HTM are indicated, along with the associated decay and half-life. Note the different range-dependences of the peak intensities.

CONCLUSIONS

Preliminary analysis of the delayed gamma spectra acquired indicates that the peaks of interest are present and exhibit the expected dependence on energy. Due to the large stopping power of heavy ion beams, this energy dependence has the potential to translate to a sub-mm range uncertainty much smaller than other uncertainties present in hadron therapy, such as CT image resolution and inherent range straggling. Further analysis is required to determine the sensitivity of HTM RV in heavy ion therapy, as well as to confirm and define the range uncertainty that can be achieved using this method. The other HTM materials studied in this experiment will be investigated for viability as well. In addition, further experiments with clinical heavy-ion beams will be necessary.

ACKNOWLEDGEMENTS

We acknowledge the support of the CIHR, NSERC and SSHRC (under Award No. NFRFE-2018-00691).

REFERENCES

1. Pompos, A., Durante, M. & Choy, H. Heavy Ions in Cancer Therapy. JAMA Oncol. 2016;2(12):1539-1540.
2. McGowan, S. E., Burnet, N. G. & Lomax, A. J. (2013). Treatment planning optimisation in proton therapy, Br J Radiol 86(1021): 20120288.
3. Kasanda, E. et al. (2020). Geant4 simulation of a new range verification method using delayed γ spectroscopy of a ^{92}Mo marker, Phys. Med. Biol. (Under Revision).
4. Burbadge, C., Kasanda, E., Bildstein, V., Dublin, G., Olaizola, B., Spyrou, A., Höhr, C. & Muecher, D. (2020). Range Verification in Proton Therapy using Delayed Gamma-Ray Spectroscopy of a ^{92}Mo Tumour Marker, Phys. Med. Biol. (Under Revision) .
5. Parodi, K. et al. (2007). Patient Study of In Vivo Verification of Beam Delivery and Range, Using Positron Emission Tomography and Computed Tomography Imaging After Proton Therapy, International Journal of Radiation Oncology*Biophysics 68(3): 920–34.
6. Tessonier T, Mairani A, Brons S, Haberer T, Debus J, Parodi K. Experimental dosimetric comparison of ^1H , ^4He , ^{12}C and ^{16}O scanned ion beams. Phys Med Biol. 2017;62(10):3958-3982. doi:10.1088/1361-6560/aa6516
7. Tarasov, O.B., Bazin, D. NIM B 266 (2008) 4657-4664;A.Gavron, Phys.Rev. C21 (1980) 230-236;http://lise.nsl.msu.edu/pace4
8. Kinsey R.R. et al, The NUDAT/PCNUDAT Program for Nuclear Data, paper submitted to the 9th International Symposium of Capture-Gamma-Ray Spectroscopy and Related Topics, Budapest, Hungary, October 1996. Data extracted from the NUDAT database, version 2.8 (June 2020), https://www.nndc.bnl.gov/nudat2/chartNuc.jsp
9. Ziegler, J. F. et al. (2010). SRIM – The stopping and range of ions in matter, Nucl. Instrum. Methods B268(11): 1818–23

CONTACT INFORMATION

Eva Kasanda: ekasanda@uoguelph.ca
Dennis Muecher: dmuecher@uoguelph.ca